Understanding the thermodynamic effects of chemically reactive working fluids in the Stirling heat pump

Aya Barakat, Jean-Noël Jaubert, Philippe Arpentinier, Pascal Tobaly, Silvia Lasala

International Journal of Refrigeration 168 (2024) 276–287

Contents lists available at ScienceDirect

International Journal of Refrigeration

journal homepage: www.elsevier.com/locate/ijrefrig

Understanding the thermodynamic effects of chemically reactive working fluids in the Stirling heat pump

Comprendre les effets thermodynamiques des fluides de travail chimiquement réactifs dans une pompe à chaleur Stirling

Aya Barakat [a], Jean-Noël Jaubert [a], Philippe Arpentinier [b], Pascal Tobaly [c], Silvia Lasala [a,*]

[a] Université de Lorraine, CNRS, LRGP, F-54000 Nancy, France
[b] Air Liquide, Innovation Campus Paris, 1 chemin de la porte des loges, 78354 Jouy-en-Josas, France
[c] Lafset (Laboratoire du froid et des systèmes énergétiques et thermiques), CNAM, HESAM Université, 292, rue Saint-Martin, Paris, 75003, France

ARTICLE INFO

Keywords:
Stirling heat pump
Chemically reactive working fluids
Chemical energy conversion
Thermodynamic analysis
Chemical equilibrium
Coefficient of performance

Mots clés:
Pompe à chaleur Stirling
Fluides actifs
Fluides réactifs chimiques
Modèle thermodynamique de gaz idéal
Équilibre chimique
Coefficient de performance

ABSTRACT

Within the realm of sustainable heating technologies, this study examines the performance of a Stirling heat pump employing chemically reactive working fluids in contrast to conventional inert counterparts. Reactive working fluids are energy vectors that enable the conversion of not only thermal but also chemical energy within the heat pump. The investigation spans a wide range of theoretical reactive gaseous mixtures, leveraging the ideal gas mixture thermodynamic model. Each fluid is characterized by an equilibrated chemical reaction, denoted as $A_{2(g)} \rightleftarrows 2A_{(g)}$, and distinguished by a set of reaction coordinates: the standard entropy change of reaction and standard enthalpy change of reaction. The chemical reaction evolution and thermodynamic properties are observed in each transformation, and the overall coefficient of performance (COP) of the system is evaluated and benchmarked against that of comparable inert working fluids. It is observed that the exothermic reaction during isothermal compression significantly increases the thermal energy supplied to the heat sink, as well as the thermal energy density per unit maximum volume, by up to 269 %, compared to an inert gas system. However, for the majority of reactive fluids studied, chemical reactions introduce irreversibility in the internal regenerator due to heat transfer across a finite temperature difference, contrary to the case of inert working fluids, penalizing the COP. Consequently, a reduction of up to 28 % in the COP is observed. Nevertheless, there exists a range of reactive fluids, characterized by reversible heat exchange in the internal regenerator, offering increased thermal energy transfer to the heat sink without compromising the COP.

1. Introduction

Space and water heating account for a substantial portion of energy consumption in buildings, particularly in cold climates, and represent the largest energy end use globally (IEA, 2022; U.S. Energy Information Administration, 2024). To date, heating remains dominated by fossil fuels and accounts for approximately 40 % of global carbon dioxide emissions (IEA, 2021). Thus, in order to achieve the Net Zero Emissions by 2050 target, greener and more efficient heating technologies should be adopted. In the context of ongoing efforts to decarbonize electricity production, heat pumps powered by green electricity have the potential to reduce carbon emissions associated with heating applications significantly.

A heat pump enables the flow of heat from a low-temperature heat source to a higher-temperature heat sink through mechanical work. The vapor compression and absorption thermodynamic cycles are the most prevalent in residential, industrial, and commercial heat pump systems. The coefficient of performance (COP) of a typical air-source residential heat pump, operating on the vapor compression cycle, is approximately four (IEA, 2022). It is observed that this COP deteriorates in cold climates.

On the other hand, a promising—though not yet widely commercialized—thermodynamic cycle for heat pumps is the reverse Stirling cycle. Indeed, refrigeration, specifically in the field of cryogenics, represents the primary industrial application of the reverse Stirling cycle

* Corresponding author.
E-mail address: silvia.lasala@univ-lorraine.fr (S. Lasala).

https://doi.org/10.1016/j.ijrefrig.2024.08.021
Received 2 May 2024; Received in revised form 21 July 2024; Accepted 25 August 2024
Available online 27 August 2024

Nomenclature

Symbols

A	Theoretical ideal gas
A_2	Dimer of ideal gas A
w	Specific work in kJ/g
q	Specific heat in kJ/g
T	Temperature
T_H	Temperature of isothermal compression
T_C	Temperature of isothermal expansion
P	Pressure
v	Specific volume
$\Delta_R H^\circ$	Standard enthalpy change of reaction at reference temperature T_0
$\Delta_R S^\circ$	Standard entropy change of reaction at reference temperature T_0
s	Specific entropy
u	Specific internal energy
z	Molar fraction of a species in the ideal gas mixture
n	Number of moles
M	Molar mass in g mol^{-1}
R	Universal gas constant

Abbreviations

COP	Coefficient of performance

Subscripts

(g)	Gaseous phase
comp	Compression
exp	Expansion
23	Isochoric cooling process (2–3)
41	Isochoric heating process (4–1)
net, in	Net input into the cycle
inert	Inert ideal gas
1	Thermodynamic point (1) in the cycle
2	Thermodynamic point (2) in the cycle
3	Thermodynamic point (3) in the cycle
4	Thermodynamic point (4) in the cycle
reg	Amount of heat exchanged in the regenerator
rej	Amount of heat rejected out of the cycle during isochoric cooling
add	Amount of heat added from an external heat source during isochoric heating
A	Corresponding to A in the ideal gas mixture
A_2	Corresponding to A_2 in the ideal gas mixture
1–2	Difference between a property at thermodynamic point (2) and at thermodynamic point (1)
2–3	Difference between a property at thermodynamic point (3) and at thermodynamic point (2)
3–4	Difference between a property at thermodynamic point (4) and at thermodynamic point (3)
4–1	Difference between a property at thermodynamic point (1) and at thermodynamic point (4)
gen, reg	Entropy generated in the regenerator
cold stream	Corresponding to the cold stream of the regenerator
hot stream	Corresponding to the hot stream of the regenerator

(Penswick et al., 2014; Radebaugh, 2009). Stirling cryocoolers are capable of efficiently and robustly achieving very low temperatures. They have demonstrated greater efficiency than vapor compression systems at such temperatures, reaching as low as 3 K. Helium is commonly reported as the primary working fluid used in Stirling cryocoolers. Other working fluids include air, nitrogen, hydrogen, and neon. Due to its high specific heat capacity, hydrogen offers the potential for a high COP in Stirling refrigerators (Tekin and Ataer, 2010); however, its practical use is limited by challenges such as leakage and high flammability.

Studies concerning the employment of the Stirling system for heating applications are limited and mainly of a theoretical nature. Tyagi et al. proposed ecological (Tyagi et al., 2002), followed by thermo-economic (Tyagi et al., 2004), optimization methods of irreversible Stirling and Ericsson heat pumps. Similarly, Ahmadi et al. proposed multi-objective thermodynamic (Ahmadi et al., 2014) and thermo-economic (Ahmadi et al., 2015) optimization methodologies of a Stirling heat pump using the non-dominated sorting genetic algorithm. Using MATLAB, Barreno et al. presented a methodology to preliminarily design a Stirling heat pump and assess the system's stability of operation for different operating conditions (Barreno et al., 2014). On the other hand, Khan et al. investigated the environmental footprint of a very high temperature Stirling heat pump using life-cycle analysis (Khan et al., 2020). Results show over 40 % reduction in the environmental impact can be achieved, compared to natural gas and oil-fired boilers. A thermodynamic model for predicting the performance of a beta-type Stirling heat pump with a rhombic drive mechanism was developed and experimentally validated by Cheng et al. (Cheng et al., 2020). The maximum difference between experimental and theoretical results was <14 %. Wang et al. studied a free-piston Stirling heat pump using the SAGE software (Wang et al., 2021). A 2409 W heating capacity and 2.41 COP were demonstrated with a heat sink and source temperatures of 40 °C and −20 °C, respectively. Kowalski et al. assessed a 10 kW Stirling heat pump using the Schmidt method (Kowalski et al., 2022). A COP ranging from 3.96 to 6.69 was obtained for heat source temperatures between 15 °C and 35 °C and heat sink temperatures ranging from 45 °C to 90 °C. In his thesis, Haywood experimentally investigated a Stirling heat pump operating with air as the working fluid (Haywood, 2004). The prototype has shown a similar COP to vapor compression systems for cold space temperatures below 0 °C, and a slightly lower COP for cold space temperatures above 0 °C.

Compared to vapor compression heat pumps, one of the main advantages of the Stirling system is the use of environmentally friendly working fluids with low or zero global warming potential. Indeed, the choice of the working fluid in the Stirling heat pump heavily influences its thermodynamic performance.

In an effort to enhance the thermodynamic performance of energy converters, novel chemically reactive working fluids are investigated. These fluids are the place of the conversion of not only thermal energy but also chemical energy. The reactive Stirling engine, operating on the "forward" Stirling thermodynamic cycle with dinitrogen tetroxide (N_2O_4) as the working fluid, has been extensively studied in the past (Metwally and Walker, 1977; Wolgemuth, 1934; Kovtun et al., 1967). It has been observed that, in a reactive Stirling engine, the internal heat exchange during the isochoric processes in the regenerator is incomplete; the heat released during isochoric cooling and the heat absorbed during isochoric heating are not equivalent due to the fluid's reactivity. Consequently, the cycle performance calculations should be modified in order to account for externally exchanged heat during the isochoric processes. The differences between the modified thermodynamic methodologies adopted justify the discrepancies in the conclusions of previous studies regarding the thermodynamic effects of utilizing chemically reactive fluids in the Stirling engine. Some studies conclude that the use of dinitrogen tetroxide in the Stirling engine leads to a significant increase in the system's work output yet a slight decrease in the thermal efficiency (Wolgemuth, 1934). Other studies claim that the

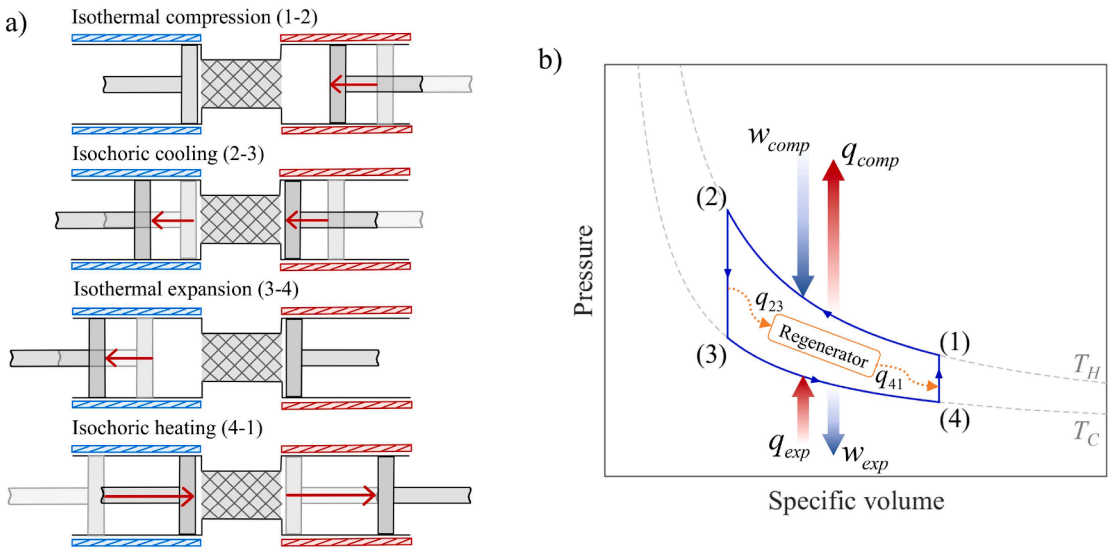

Fig. 1. Schematic representation of the four sequential processes of a heat pump operating on the reverse Stirling cycle (Fig. a); P-v diagram of an ideal Stirling heat pump operating with an inert ideal gas (Fig. b).

effective efficiency of the Stirling engine significantly increases with the use of dinitrogen tetroxide as the working fluid (Kovtun et al., 1967). However, practical applications of N_2O_4 are limited due to corrosion and toxicity issues.

In response, in a preceding publication (Barakat et al., 2024), the authors investigated a wide range of theoretical chemically reactive working fluids in a Stirling engine operating between 400 K and 900 K. Since the theoretical thermal efficiency of an inert ideal Stirling engine amounts to that of a Carnot engine operating between the same heat source and sink temperatures, using reactive working fluids does not offer an advantage in terms of efficiency. Indeed, for the majority of reactive fluids studied, the efficiency is significantly lower than that of a comparable inert fluid system, primarily due to incomplete irreversible internal regeneration. Furthermore, the specific expansion work generated, specific compression work required, and net specific work output of the cycle are lower for the majority of reactive fluids considered. However, certain reactive fluids–characterized by higher compression and expansion ratios–achieve a maximum of 5 % increase in the specific work output of the cycle, compared to inert fluids. The limited improvement in the net specific work output can be attributed to the narrow pressure ranges considered in the study of Barakat et al. (2024) in order to comply with the ideal gas thermodynamic assumption adopted.

On the contrary, to the authors' knowledge, the study of chemically reactive working fluids in a heat pump operating on the reverse Stirling cycle is absent from the literature. Hence, this work is aimed at investigating the thermodynamic effects of utilizing chemically reactive working fluids in a Stirling heat pump system. A wide range of theoretical reactive gaseous mixtures are investigated in a system operating between 400 K and 900 K, the same range considered in the Stirling engine study Barakat et al. (2024). Each of these fluids is characterized by a theoretical equilibrated chemical reaction, identified by a unique set of reaction coordinates (the standard enthalpy and entropy change of reaction). Furthermore, these fluids are modeled as ideal gas mixtures that undergo compositional changes under the influence of thermodynamic transformations throughout the reverse Stirling cycle. Consequently, the behavior of each reactive fluid is assessed in each of the heat pump's units, the overall performance of the reactive system is evaluated, and the results are benchmarked against those of comparable theoretical inert fluids.

Similar methodologies have been employed by the authors to investigate reactive Brayton engines (Lasala et al., 2021), heat pumps based on the reverse Brayton cycle (Barakat et al., 2022), and, as aforementioned, Stirling engines (Barakat et al., 2024). The work conducted in these studies falls within the scope of the REACHER research project (Lasala, 2022), which is funded by the European Research Council, with the objective of designing and investigating innovative reactive working fluids for thermodynamic cycles (Lasala et al., 2024).

2. Methodology

This section introduces the Stirling heat pump system under investigation in this study (Section 2.1), outlines the methodology employed to model the theoretical reactive working fluids within the system (Section 2.2), and describes the approach followed to conduct the thermodynamic analysis of the Stirling heat pump (Section 2.3).

2.1. The Stirling heat pump

The reciprocating Stirling heat pump operates on the reverse Stirling cycle, which comprises four sequential processes: isothermal compression at a high temperature T_H (1–2), during which compression work (w_{comp}) is input and heat is released to the heat sink $\left(q_{comp}\right)$; isochoric cooling (2–3); isothermal expansion at a low temperature T_C (3–4), during which expansion work (w_{exp}) is generated and heat is absorbed from a heat source $\left(q_{exp}\right)$; and isochoric heating (4–1). Theoretically, isochoric cooling and heating occur within the internal regenerator. During isochoric cooling, the fluid cools down as it passes through the regenerator which retains the heat released (q_{23}). Conversely, during isochoric heating, the fluid heats up by reabsorbing the heat stored in the regenerator (q_{41}). Fig. 1(a) schematically illustrates the four processes. The pressure-volume $(P-v)$ diagram of an ideal Stirling heat pump operating with an inert ideal gas is presented in Fig. 1(b).

In this work, the system operates with an ideal gas or gaseous mixture. The system is assumed to be devoid of any mechanical or thermal losses.

The COP of a Stirling heat pump operating with an inert fluid can be calculated according to the following equation:

$$COP = \frac{q_{comp}}{w_{net,in}} \tag{1}$$

Where $w_{net,in}$ is the net specific work input to the cycle and can be calculated according to:

Table 1
Equations used to calculate the work and heat quantities in the heat pump cycle.

Calculated energy type	Equation	
Isothermal compression (1–2) specific heat output, q_{comp} [kJ/g]	$q_{comp} = T_H(s_1 - s_2)$ Where s is the specific entropy of the reactive gaseous mixture	(6)
Isothermal expansion (3–4) specific heat input, q_{exp} [kJ/g]	$q_{exp} = T_C(s_4 - s_3)$	(7)
Isothermal compression (1–2) specific work input, w_{comp} [kJ/g]	$w_{comp} = q_{comp} + (u_2 - u_1)$ Where u is the specific internal energy of the reactive gaseous mixture	(8)
Isothermal expansion specific (3–4) work output, w_{exp} [kJ/g]	$w_{exp} = q_{exp} + (u_3 - u_4)$	(9)
Specific heat released during isochoric cooling (2–3), q_{23} [kJ/g]	$q_{23} = u_2 - u_3$	(10)
Specific heat absorbed during isochoric heating (4–1), q_{41} [kJ/g]	$q_{41} = u_1 - u_4$	(11)

Table 2
Six possible sets of heat quantities exchanged during isochoric processes (2–3) and (4–1) as a result of using chemically reactive gaseous mixtures in the Stirling heat pump.

	Case I: $q_{23} = q_{41}$	Case II: $q_{23} > q_{41}$	Case III: $q_{41} > q_{23}$
No temperature cross as the minimum of q_{23} and q_{41} (q_{reg}) is exchanged between the two streams	$q_{23} = q_{reg}$ $q_{41} = q_{reg}$ $q_{rej} =$ $q_{add} = 0$	$q_{23} = q_{reg} +$ q_{rej} $q_{41} = q_{reg}$ $q_{add} = 0$	$q_{23} = q_{reg}$ $q_{41} = q_{reg} +$ q_{add} $q_{rej} = 0$
Temperature cross as the minimum of q_{23} and q_{41} is exchanged between the two streams	$q_{23} =$ $q_{reg} + q_{rej}$ $q_{41} =$ $q_{reg} + q_{add}$ $q_{rej} = q_{add}$	$q_{23} = q_{reg} +$ q_{rej} $q_{41} = q_{reg} +$ q_{add} $q_{rej} > q_{add}$	$q_{23} = q_{reg} +$ q_{rej} $q_{41} = q_{reg} +$ q_{add} $q_{add} > q_{rej}$

$$w_{net.in} = w_{comp} - w_{exp} \tag{2}$$

Therefore, for any inert ideal gas, the COP of an ideal Stirling heat pump corresponds to that of a reverse Carnot cycle–a theoretical upper limit for the COP of any heat pump operating between the considered heat reservoirs:

$$COP_{inert} = \frac{T_H}{T_H - T_C} \tag{3}$$

Given the operating temperatures considered ($T_H = 900$ K and $T_C = 400$ K), the COP of the inert fluids in this study amounts to 1.8, the highest achievable COP. Indeed, in the case of a Stirling heat pump operating with an ideal gas, heat transfer in the internal regenerator is reversible, as there is no temperature difference between streams (2–3) and (4–1) throughout the exchange.

On the other hand, utilizing reactive gases, rather than inert ones, in the Stirling heat pump leads to compositional changes in the fluid, and, potentially, heat exchange across a finite temperature difference in the internal regenerator. For these fluids, the internal regenerator is no longer reversible. Consequently, the heat pump can not be referred to as ideal.

2.2. Theoretical chemically reactive gases

A range of theoretical chemically reactive gaseous mixtures is considered in this study as working fluids in the Stirling heat pump. Each of these fluids is characterized by the following equilibrated chemical reaction:

$$A_{2(g)} \rightleftarrows 2A_{(g)} \tag{4}$$

Where A is a theoretical chemical species, and A_2 is the corresponding dimer. These two species compose the reactive working fluid throughout the cycle.

The methodology for modeling the reactive gaseous mixtures composed of A and A_2, and for evaluating their thermodynamic properties throughout the Stirling heat pump cycle, is detailed in a preceding publication on chemically reactive Stirling engines (Barakat et al., 2024).

Each reactive fluid is characterized by a unique set of the reaction coordinates: the standard entropy change of reaction $\Delta_R S^\circ$, and the standard enthalpy change of reaction $\Delta_R H^\circ$. Hence, each set of these coordinates $(\Delta_R S^\circ, \Delta_R H^\circ)$ identifies a unique reactive gaseous mixture.

2.3. Thermodynamic analysis of the Stirling heat pump

In a preceding work (Barakat et al., 2024), the authors adopted a similar methodology to assess the performance of a chemically reactive Stirling engine operating on the forward Stirling cycle, in contrast to the reverse cycle considered in the current work. As in the study of chemically reactive Stirling engines (Barakat et al., 2024), the thermodynamic analysis is performed for the following operating conditions: the system's lowest pressure $P_4 = 0.1$ bar, highest pressure $P_2 = 0.61$ bar, low temperature $T_C = 400$ K, and high temperature $T_H = 900$ K (refer to Fig. 1). Pressures P_1 and P_3 are unknown. For each reactive fluid considered, P_1 and P_3 can be calculated by solving the following system of equations:

$$\begin{cases} v_1(T_H, P_1) = v_4(T_C, P_4) \\ v_3(T_C, P_3) = v_2(T_H, P_2) \end{cases} \tag{5}$$

Note that the specific volume of the gaseous mixture, v, is calculated as a function of T and P using the ideal gas equation of state after determining the mixture's composition, according to chemical equilibrium. The full methodology is detailed in a previous article (Barakat et al., 2024).

After determining the unknown pressures, the thermodynamic properties at each state of the cycle can be evaluated. Subsequently, the heat and work quantities, illustrated in Fig. 1(b), can be calculated according to the equations presented in Table 1.

Unlike the case of inert ideal gases, certain chemically reactive working fluids could lead to incomplete internal regeneration; that is, the total heat released during isochoric cooling q_{23} and that absorbed during isochoric heating q_{41} are not equivalent. For some reactive fluids, q_{23} could be greater than q_{41}, or vice versa. Theoretically, the heat exchanged in the regenerator, q_{reg}, would be determined as the minimum value between q_{23} and q_{41}, $q_{reg} = \min(q_{23}, q_{41})$. In the case where q_{23} is greater than q_{41}, the excess heat released during isochoric cooling q_{rej} $\left(q_{rej} = q_{23} - q_{reg} \text{ where } q_{reg} = q_{41}\right)$ is rejected out of the cycle into an additional heat sink. On the contrary, in the case where q_{41} exceeds q_{23}, the latter proves insufficient for heating the cold stream, resulting in a heat deficit. Consequently, an additional heat source is required during isochoric heating to supply the shortfall, q_{add}, which corresponds to the difference between q_{41} and q_{23}: $q_{add} = q_{41} - q_{reg}$ where $q_{reg} = q_{23}$.

However, there are cases where q_{reg} is less than the minimum of q_{23} and q_{41}. This is due to the presence of a temperature cross in the regenerator as the two streams exchange the heat quantity that is equivalent to the minimum of q_{23} and q_{41}, which demands reducing the amount of heat exchanged. In this case, both an additional heat sink and source are needed during the isochoric processes, respectively. Table 2 summarizes the possible heat quantities exchanged during the isochoric processes as an effect of utilizing chemically reactive working fluids.

Accordingly, in the case of a reactive Stirling heat pump, the equation to calculate the COP should be adjusted to account for any heat addition from an external source during isochoric heating (4–1), as presented in Eq. (12). It is assumed that in cases where an external heat supply is required during isochoric heating, this supplemental heat (q_{add}) is sourced from the heat released during isothermal compression

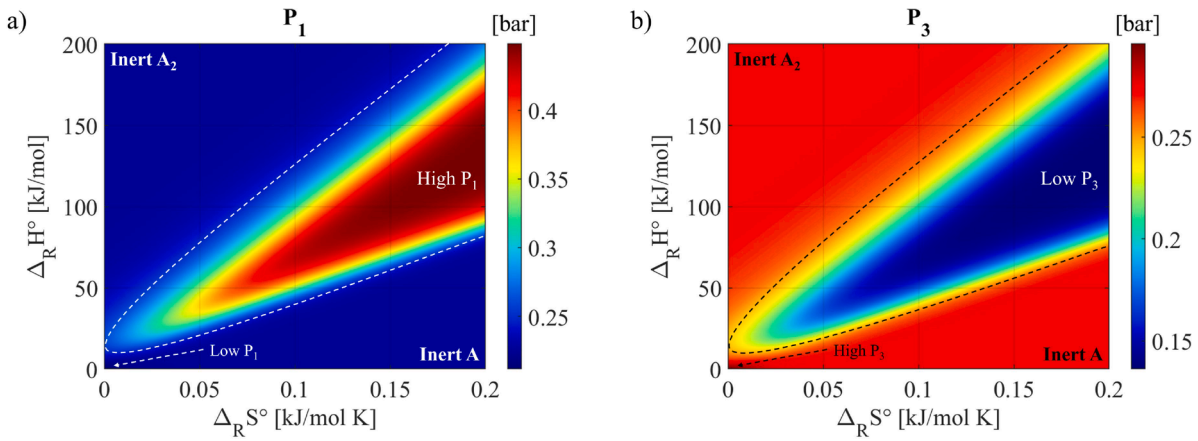

Fig. 2. Pressure at the isothermal compression process inlet, P_1 (Fig. a), and pressure at the isothermal expansion process inlet, P_3 (Fig. b), for each studied theoretical reactive working fluid $(\Delta_R S^\circ, \Delta_R H^\circ)$.

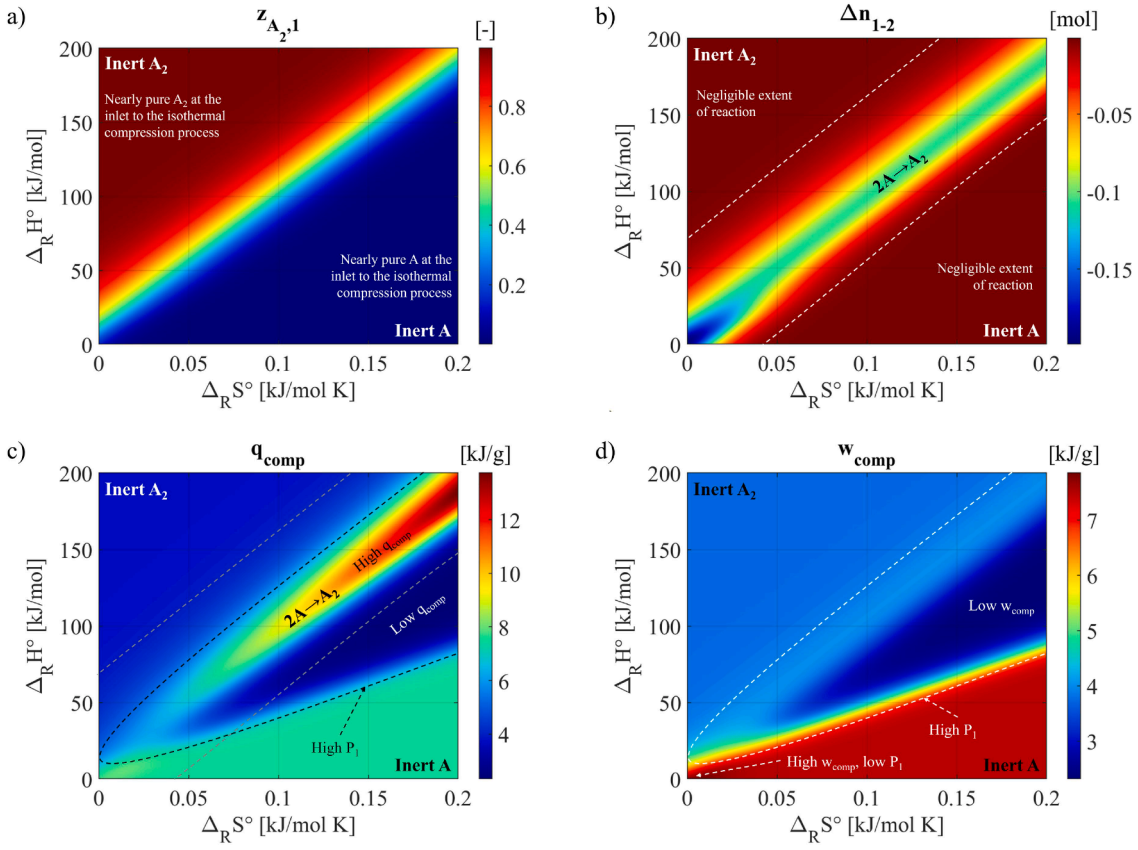

Fig. 3. The behavior of each studied theoretical reactive working fluid $(\Delta_R S^\circ, \Delta_R H^\circ)$ during isothermal compression. $z_{A_2,1}$ (Fig. a); $\Delta n_{1-2} = n_2 - n_1$ (Fig. b); q_{comp} (Fig. c); and w_{comp} (Fig. d).

$\left(q_{comp}\right)$, decreasing the heat provided to the heat sink.

$$COP = \frac{q_{comp} - q_{add}}{w_{net,in}} \tag{12}$$

To ensure completeness, it is noted that all calculations were conducted using Fortran and MATLAB codes developed by the authors.

3. Results and discussion

In this section, the properties of each reactive fluid are analyzed during isothermal compression, isochoric cooling, isothermal expansion, and isochoric heating. The heat and work quantities involved are presented, and the overall cycle performance (COP) is discussed. The results are benchmarked against those of comparable theoretical inert working fluids, A and A_2.

The unknown pressures, P_1 and P_3, are calculated according to the methodology presented in Section 2.3 for all the reactive fluids considered, as shown in Fig. 2. Hence, each point in the colormaps $(\Delta_R S^\circ, \Delta_R H^\circ)$ corresponds to a unique theoretical reactive fluid.

As observed in previous works (Barakat et al., 2024; Lasala et al., 2021; Barakat et al., 2022), the fluids at the top-left and bottom-right corners of the colormaps resemble the properties and behavior of inert

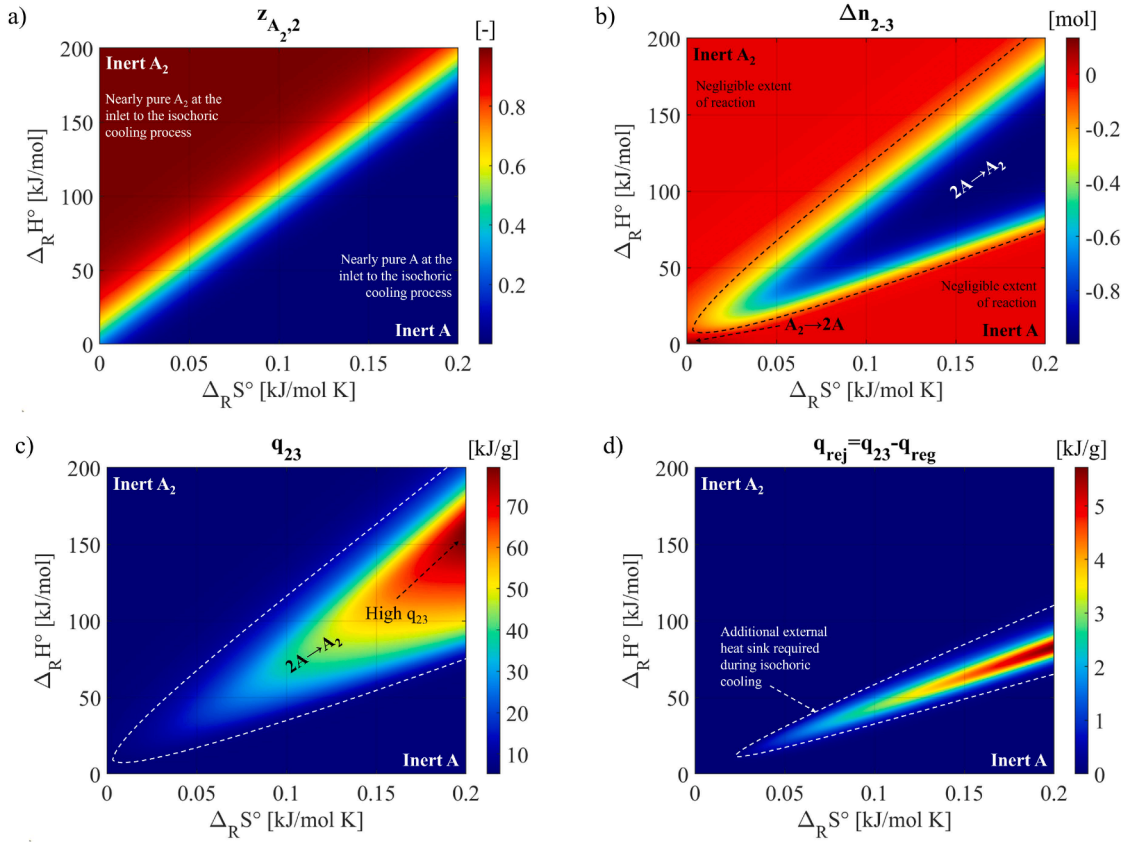

Fig. 4. The behavior of each studied theoretical reactive working fluid $(\Delta_R S°, \Delta_R H°)$ during isochoric cooling. $z_{A_2,2}$ (Fig. a); $\Delta n_{2-3} = n_3 - n_2$ (Fig. b); q_{23} (Fig. c); and q_{rej} (Fig. d).

fluids A_2 and A, respectively. Thus, these fluids are used as a benchmark to assess the behavior of reactive working fluids that correspond to intermediate values of $(\Delta_R S°, \Delta_R H°)$.

Observing Fig. 2(a), for the majority of the reactive fluids, the pressure at the inlet to the isothermal compression process, P_1, is higher than that of inert fluids A and A_2, reaching approximately 0.45 bar. This leads to a lower compression ratio (P_2/P_1) with a minimum of 1.36 rather than 2.72 which corresponds to the compression ratio of inert fluids. Exceptionally, for low values of the reaction coordinates $(\Delta_R S°, \Delta_R H°)$, P_1 is lower than that of A and A_2, reaching a minimum of 0.21 bar and resulting in a higher compression ratio for the corresponding fluids (up to 2.89).

On the other hand, observing Fig. 2(b), for the majority of reactive fluids, the pressure at the inlet to the isothermal expansion process, P_3, is lower than that of the inert fluids, reaching a minimum of approximately 0.14 bar. This results in a low expansion ratio (P_3/P_4) for the majority of reactive fluids with a minimum of 1.36. Exceptionally, for low values of $\Delta_R S°$ and $\Delta_R H°$, P_3 is higher than that of A and A_2, reaching 0.3 bar and resulting in a high expansion ratio (up to 2.96).

Note that the calculated pressure values, P_1 and P_3, highly depend on the chemical reaction evolution in the fluid. For example, the pressure at the inlet to the isothermal compression process, P_1, is calculated using Eq. (5). Therefore, the chemical reaction evolution during isochoric heating (4–1) impacts the value of P_1. During this process, the temperature of the system increases from T_C to T_H at constant volume. The temperature rise increases the pressure of the fluid. If the fluid undergoes a dissociation endothermic reaction, the number of the moles in the system increases as a consequence of the reaction, elevating the pressure of the fluid at each temperature, compared to an inert fluid where no reaction takes place during the process. In contrast, if the fluid undergoes an association exothermic reaction, the number of moles in the mixture decreases, decreasing its pressure. The same analysis can be performed for the pressure at the inlet to the isothermal expansion process, P_3. The chemical reaction evolution during each thermodynamic transformation is presented in the following sections.

After calculating the unknown pressures, P_1 and P_3, the exchanged heat and work quantities can be investigated.

3.1. Isothermal compression

In order to investigate the reaction evolution in the studied fluids during isothermal compression, the equilibrium molar fraction of A_2 at the inlet, $z_{A_2,1}$, as well as the variation in the number of moles during the process, $\Delta n_{1-2} = n_2 - n_1$, are presented in Figs. 3(a) and 3(b), respectively. Furthermore, the specific heat released to the heat sink at T_H, q_{comp}, and the specific compression work input during the process, w_{comp}, are given in Figs. 3(c) and 3(d), respectively.

Observing Fig. 3(a), the reactive fluid is mainly composed of A for high values of $\Delta_R S°$ and low values of $\Delta_R H°$, A_2 for low values of $\Delta_R S°$ and high values of $\Delta_R H°$, and a mixture of the two gases for intermediate values of the reaction coordinates $(\Delta_R S°, \Delta_R H°)$ at the inlet to the isothermal compression process.

During the isothermal compression process (1–2), the reaction shifts in the exothermic association direction, as presented in Fig. 3(b). This is due to the increase in the system's pressure at a constant temperature during isothermal compression, leading to a reaction shift towards the decreasing number of moles, in accordance with the law of mass action (Koudriavtsev et al., 2011). The variation in the number of moles becomes more prominent for low values of the reaction coordinates $(\Delta_R S°, \Delta_R H°)$. Note that the variation in the number of moles of a given working fluid $(\Delta n \neq 0)$—as presented in Fig. 3(b)—during a thermodynamic transformation signifies that a chemical reaction has taken place during the process.

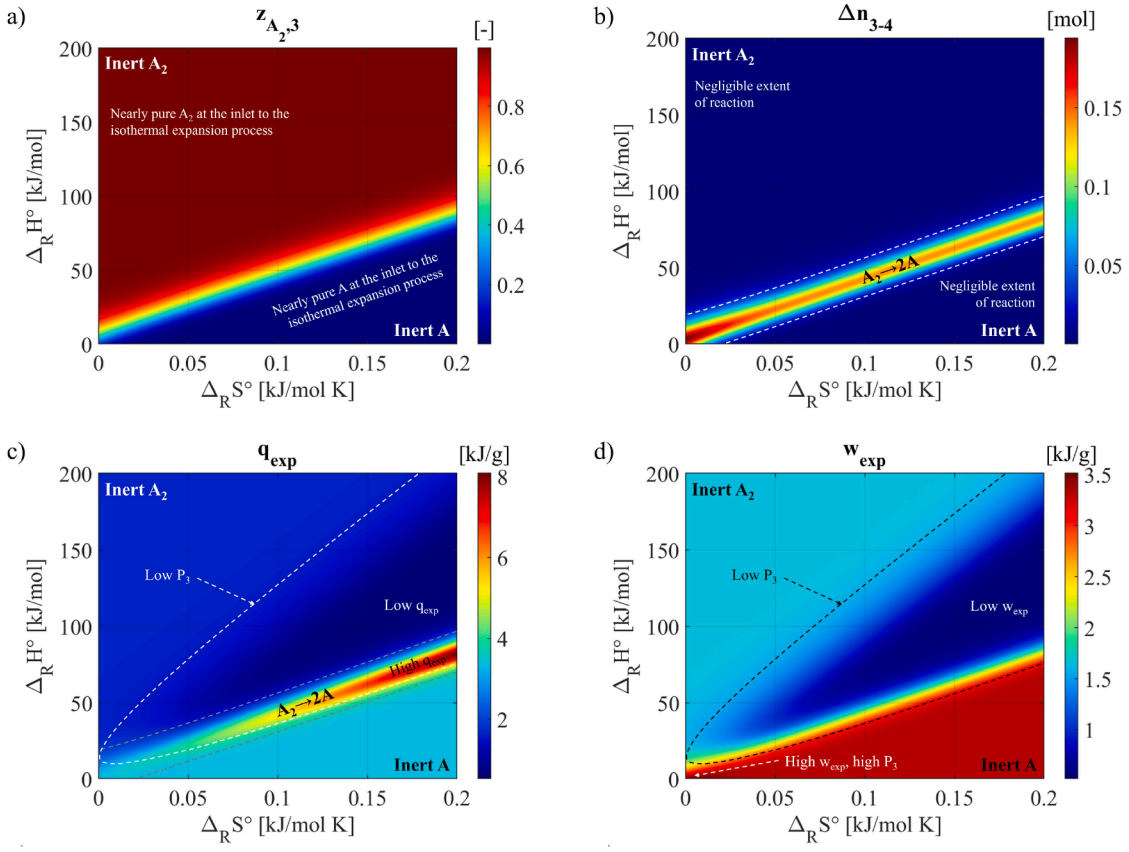

Fig. 5. The behavior of each studied theoretical reactive working fluid $(\Delta_R S°, \Delta_R H°)$ during isothermal expansion.$z_{A_2,3}$ (Fig. a); $\Delta n_{3-4} = n_4 - n_3$ (Fig. b); q_{exp} (Fig. c); and w_{exp} (Fig. d).

The effect of the exothermic reaction during compression can be observed in the specific heat released to the heat sink, as presented in Fig. 3(c). For some reactive fluids, the reaction leads to significantly higher values of q_{comp} reaching 13.8 kJ/g compared to 7.5 kJ/g and 3.7 kJ/g corresponding to inert fluids A and A_2, respectively. This signifies up to 269 % increase in the specific heat provided to the heat sink, q_{comp}, compared to an inert Stirling heat pump cycle. For a reactive Stirling heat pump utilizing fluids characterized by high q_{comp} values, less fluid mass is required to release the same amount of thermal energy (in joules) compared to a system operating with inert fluids. Conversely, for the other reactive fluids where the reaction is not prominent, q_{comp} is lower than that of the inert fluids with a minimum of 2.3 kJ/g. This can be attributed to the lower compression ratio (P_2/P_1), as presented in Fig. 2(a).

Similarly, observing Fig. 3(d), for the reactive fluids characterized by a low compression ratio compared to inert fluids A and A_2, the compression work w_{comp} input to the cycle is low. This signifies up to 38 % and 69 % decrease in w_{comp} compared to A_2 and A, respectively. However, for low values of $(\Delta_R S°, \Delta_R H°)$, the compression ratio of the reactive fluids is higher than that of the inert fluids, leading to higher specific compression work with a maximum of 7.88 kJ/g.

3.2. Isochoric cooling

In this section, the behavior of the reactive fluid is investigated during isochoric cooling. The equilibrium molar fraction of A_2 at the inlet to the process, $z_{A_2,2}$, variation in the number of moles, $\Delta n_{2-3} = n_3 - n_2$, total specific heat released during isochoric cooling q_{23}, and fraction of q_{23} that is rejected to an additional external heat sink, q_{rej}, are given in Fig. 4.

During isochoric cooling, the temperature of the reactive fluid decreases from T_H to T_C at a constant volume. According to the van't Hoff equation (Kemp, 1987), as the system's temperature decreases at a constant pressure, the reaction shifts in the exothermic association direction, $2A_{(g)} \rightarrow A_{2(g)}$. Observing Fig. 2(b), during the isochoric cooling process (2–3), the fluid's pressure also decreases from P_2, at 0.61 bar, to P_3. Hence, according to the law of mas action, as the pressure of a reactive fluid decreases at a constant temperature, the reaction shifts in the dissociation endothermic direction, $A_{2(g)} \rightarrow 2A_{(g)}$. Therefore, the effects of temperature and pressure on the reaction evolution during process (2–3) are opposite. Observing Fig. 4(b), the reaction shifts in the direction of decreasing number of moles, $2A_{(g)} \rightarrow A_{2(g)}$, for the majority of the reactive fluids. Therefore, the effect of temperature is more pronounced for the corresponding fluids. On the other hand, for low values of the reaction coordinates $(\Delta_R S°, \Delta_R H°)$, the reaction shifts in the opposite endothermic direction, where the pressure effect is more pronounced.

The effect of the exothermic association reaction can be observed in Fig. 4(c), significantly increasing the total heat rejected during isochoric cooling, q_{23}. For certain reactive fluids where the association reaction is most prominent, q_{23} reaches approximately 79.6 kJ/g compared to 6.2 kJ/g and 5.2 kJ/g corresponding to A and A_2, respectively. On the contrary, for low values of $(\Delta_R S°, \Delta_R H°)$, the endothermic reaction contributes to cooling the fluid down during isochoric cooling, and the specific heat released is comparable to that of A and A_2.

In the cases where the total heat rejected during isochoric cooling is greater than the heat exchanged in the internal regenerator $\left(q_{23} > q_{reg}\right)$ due to the chemical reaction, the excess heat $\left(q_{rej} = q_{23} - q_{reg}\right)$ is rejected out of the cycle into an additional heat sink during process (2–3). Note that q_{reg} is evaluated either as the minimum value among q_{23} and q_{41}, $\min(q_{23}, q_{41})$, in the absence of a temperature cross in the regen-

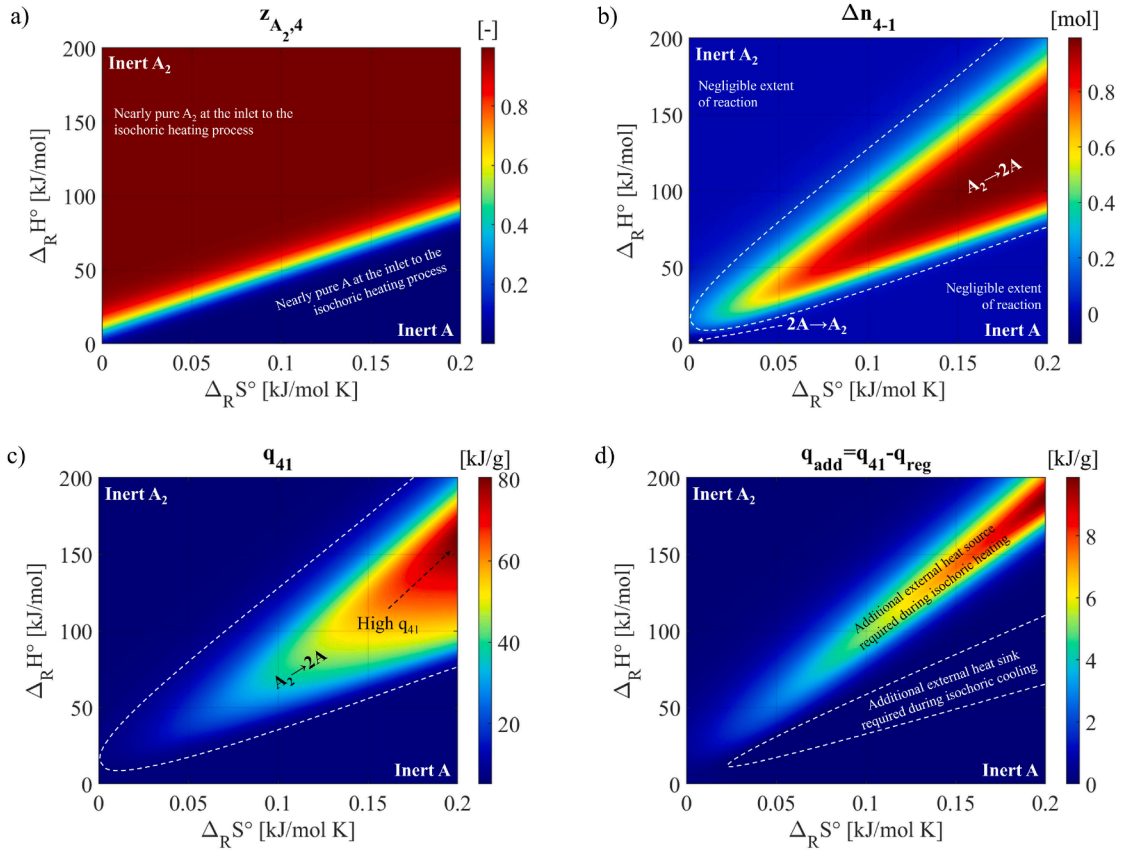

Fig. 6. The behavior of each studied theoretical reactive working fluid $(\Delta_R S°, \Delta_R H°)$ during isochoric heating. $z_{A_2,4}$ (Fig. a); $\Delta n_{4-1} = n_1 - n_4$ (Fig. b); q_{41} (Fig. c); and q_{add} (Fig. d).

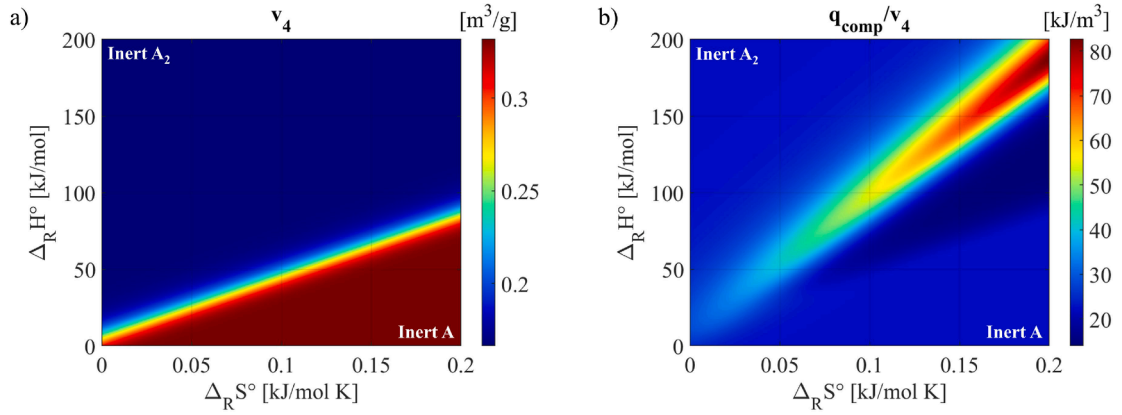

Fig. 7. Maximum volume of the Stirling machine, v_4 (Fig. a), and the specific heat supplied to the heat sink per unit maximum volume, q_{comp}/v_4 (Fig. b), for each studied theoretical reactive working fluid $(\Delta_R S°, \Delta_R H°)$.

erator, or using numerical methods in the presence of a temperature cross, according to the methodology in Section 2.3. For the reactive fluids where q_{rej} amounts to zero, as depicted in Fig. 4(d), heat rejection out of the cycle exclusively takes place during the isothermal compression process; there is no need for an additional heat sink during process (2–3). For certain reactive fluids, q_{rej} reaches up to approximately 29 % of the corresponding q_{23}.

3.3. Isothermal expansion

After the reactive gaseous mixture cools down isochorically, it undergoes isothermal expansion at T_C where heat is absorbed from the heat source, q_{exp}, and expansion work is generated, w_{exp}, as presented in Fig. 5. The equilibrium molar fraction of A_2 at the inlet to isothermal expansion, $z_{A_2,3}$, and variation in the number of moles, $\Delta n_{3-4} = n_4 - n_3$, are also given in Fig. 5.

Observing Figs. 5(a) and 5(b), the reaction shifts in the dissociation endothermic direction during isothermal expansion due to the pressure decrease at a constant temperature (in accordance with the law of mass action). The reaction becomes more important for low values of the reaction coordinates $(\Delta_R S°, \Delta_R H°)$.

The effect of the endothermic reaction can be observed in Fig. 5(c) leading to an increase in the heat absorbed from the heat sink at T_C, q_{exp}, reaching up to approximately 8.1 kJ/g for certain reactive fluids,

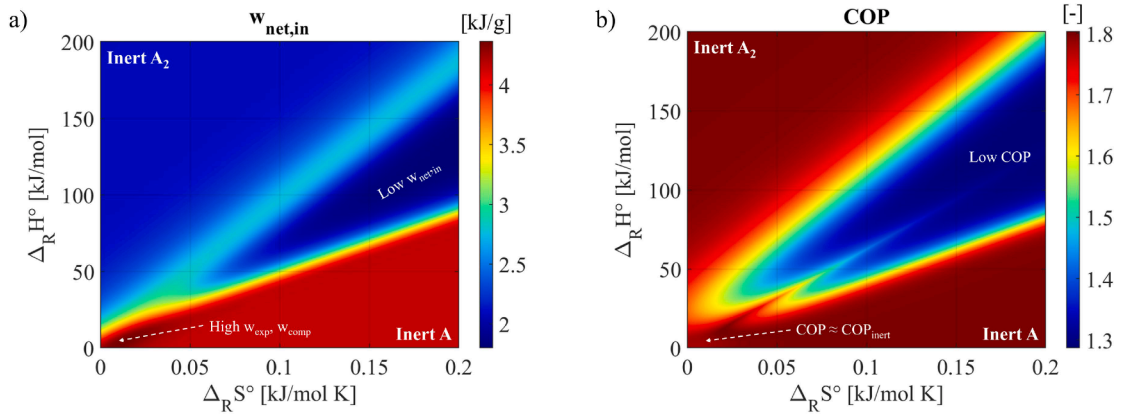

Fig. 8. Net specific work input to the cycle, $w_{net,in} = w_{comp} - w_{exp}$ (Fig. a), and the heat pump's coefficient of performance calculated using Eq. (12), *COP* (Fig. b), for each studied theoretical reactive working fluid $(\Delta_R S°, \Delta_R H°)$.

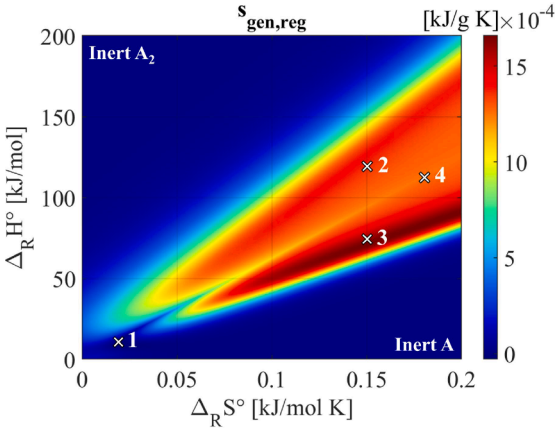

Fig. 9. The entropy generated in the internal regenerator $s_{gen,reg}$ for each studied theoretical reactive working fluid $(\Delta_R S°, \Delta_R H°)$.

compared to 3.3 kJ/g and 1.7 kJ/g absorbed by A and A_2, respectively. On the other hand, for other reactive fluids where the reaction is not prominent, q_{exp} is lower than that of the inert fluids. This can be attributed to the low expansion ratio (P_3/P_4) of the corresponding fluids; refer to Fig. 2(b).

The low expansion ratio, characterizing the majority of the reactive fluids, penalizes the expansion work generated w_{exp}. Exceptionally, for low values of the reaction coordinates $(\Delta_R S°, \Delta_R H°)$ where the expansion ratio is higher than that of inert fluids A and A_2, w_{exp} is high, reaching 3.52 kJ/g compared to 3.3 kJ/g and 1.7 kJ/g generated by A and A_2, respectively.

3.4. Isochoric heating

The equilibrium molar fraction of A_2 at the inlet to the isochoric heating process, $z_{A_2,4}$, variation in the number of moles, $\Delta n_{4-1} = n_1 - n_4$, total specific heat absorbed during isochoric heating, q_{41}, and fraction of q_{41} that is absorbed from an additional external heat source, q_{add}, are presented in Fig. 6.

As presented in Figs. 6(a) and 6(b), for the majority of the reactive fluids, the reaction shifts in the endothermic dissociation direction, $A_{2(g)} \rightarrow 2A_{(g)}$, during isochoric heating. Exceptionally for low values of $(\Delta_R S°, \Delta_R H°)$, the reaction shifts in the opposite direction, $2A_{(g)} \rightarrow A_{2(g)}$.

The endothermic reaction during isochoric heating induces an unfavorable cooling effect in the fluid, leading to a significant increase in the total heat required, q_{41}, to isochorically heat the fluid to the heat sink temperature, T_H. This can be observed in Fig. 6(c), where q_{41} reaches approximately 80.8 kJ/g, compared to 6.2 kJ/g and 5.2 kJ/g absorbed by A and A_2, respectively.

In the case where the heat available in the regenerator $\left(q_{reg}\right)$ is less than that needed to heat the fluid during process (4–1), q_{41}, additional heat is absorbed from an external heat source (q_{add}), as presented in Fig. 6(d). For certain reactive fluids, q_{add} amounts to approximately 26 % of the total heat absorbed during isochoric heating. Note that for the fluids that do not require an additional heat source during process (4–1), where q_{reg} is sufficient to isochorically heat the fluid, heat input to the cycle exclusively takes place during isothermal expansion.

Fig. 6(d) also highlights the fluids that require an additional heat sink during isochoric cooling. For the majority of the reactive fluids, either a heat source or a heat sink is required during one of the isochoric processes. However, for a narrow range of reactive fluids, both an additional heat source and sink are needed during the isochoric processes. The latter occurs for low values of the reaction coordinates where the two zones displayed in Fig. 6(d) intersect. Furthermore, there exists another narrow range of reactive fluids where neither a heat source nor a heat sink is needed during any of the isochoric processes. This range lies between the two marked zones in the colormap in Fig. 6(d).

Indeed, the system's maximum volume, v_4, that is calculated as a function of the temperature and pressure using the ideal gas equation of state in Eq. (13) at thermodynamic state (4), serves as indicator of the heat pump's size.

$$v = \frac{RT}{MP} \tag{13}$$

Where R is the universal gas constant, and M is the molar mass of the gaseous mixture.

The temperature and pressure values at thermodynamic state (4) are fixed for all the theoretical working fluids considered, as detailed in Section 2.3. Therefore, variations in the calculated specific volumes of inert and reactive fluids are due to differences in the molar mass, as per Eq. (13). Fig. 7(a) presents the Stirling machine's maximum volume, v_4.

On the other hand, the heat supplied to the heat sink, q_{comp}, per unit maximum volume, v_4, can be calculated in order to better understand the gain in thermal energy density of a reactive Stirling heat pump compared to an inert counterpart, as depicted in Fig. 7(b).

Note that the molar mass of the reactive mixture varies between that of A (1 g mol^{-1}) and A_2 (2 g mol^{-1}). Therefore, for the same temperature and pressure, the specific volume of the reactive mixture also varies between that of A and A_2, depending on the molar mass.

Observing Fig. 7(a), the maximum volume, v_4, corresponding to the majority of reactive fluids is comparable to that of inert fluid A_2. On the other hand, the thermal energy density of certain reactive fluids–calculated by the ratio of the specific heat supplied to the heat sink per unit maximum volume–is significantly higher than that of the inert

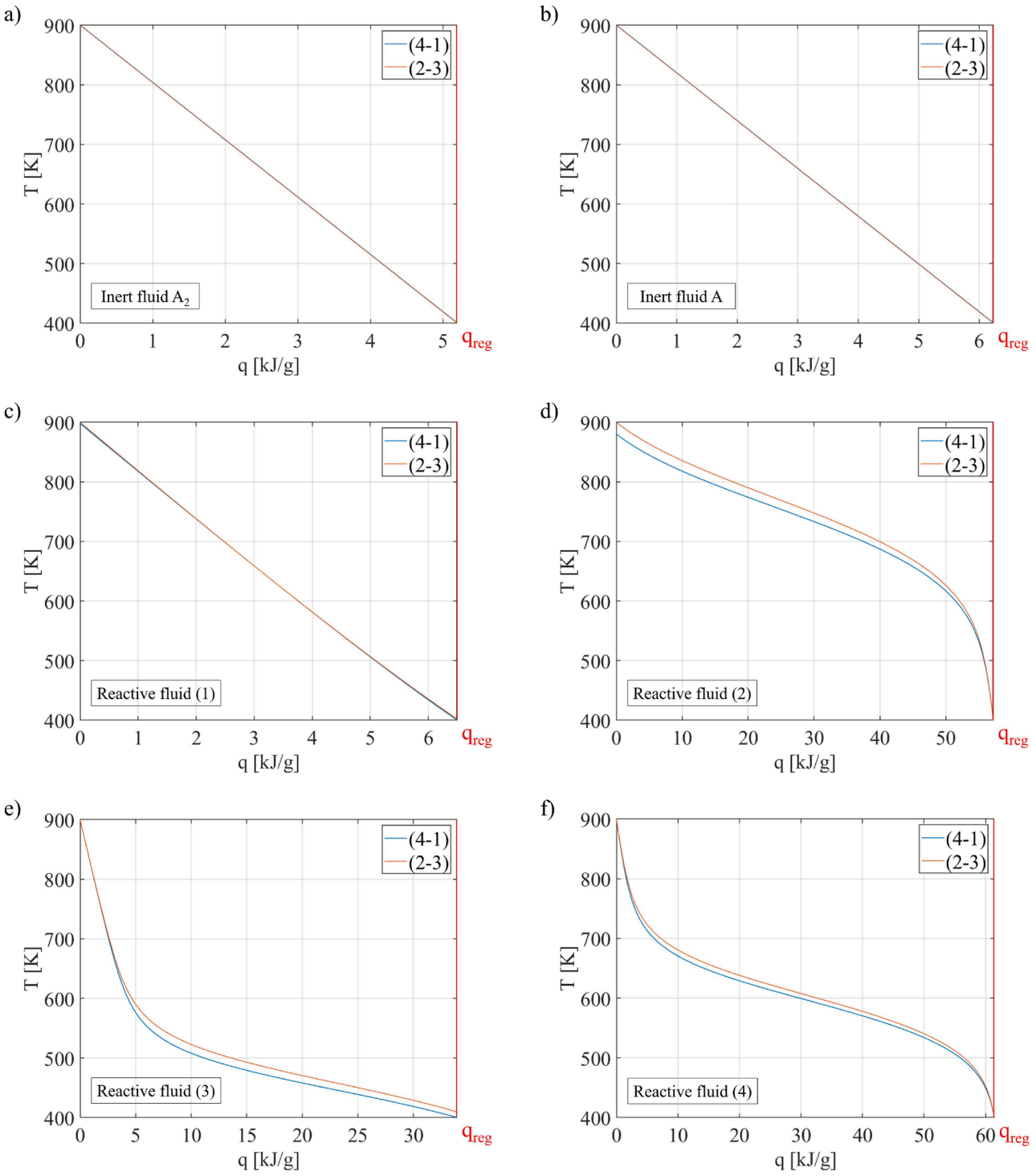

Fig. 10. Internal regenerator T-q diagrams for inert fluids A and A_2, as well as the four reactive fluids marked in Fig. 9.

fluids. For example, the reactive fluid identified by the reaction coordinates ($\Delta_R S^\circ = 0.2$ kJ/mol K, $\Delta_R H^\circ = 187$ kJ/mol) is characterized by an energy density that is equivalent to 83 kJ /m^3, 269 % higher than the thermal energy density of A and A_2. Therefore, the corresponding reactive Stirling heat pump can be competitive in applications where size is a critical factor.

3.5. Overall cycle performance

The net specific work input, calculated using Eq. (2), is presented in Fig. 8(a). Additionally, the COP of the heat pump is given in Fig. 8(b).

For the majority of reactive fluids considered, the required net specific work input to the cycle ($w_{net,in}$) is less than that corresponding to inert fluid A with a minimum of 1.8 kJ/g, as depicted in Fig. 8(a). For low values of the reaction coordinates ($\Delta_R S^\circ$, $\Delta_R H^\circ$), where both the specific compression and expansion work are relatively high, $w_{net,in}$ is also high, reaching 4.37 kJ/g compared to 4.16 kJ/g corresponding to inert fluid A. This signifies a slight increase of 5 %. The fluids characterized by this $w_{net,in}$ offer a COP that is comparable to those of inert fluids A and A_2, as presented in Fig. 8(b). On the contrary, for the

majority of reactive fluids, the COP is less than that of the inert fluids. As expected, the COP of inert fluids given in Eq. (3), amounting to the COP of a Carnot heat pump operating between T_C and T_H, represents an upper limit to the COP of all the reactive heat pumps studied. Nevertheless, when comparing Fig. 3(c) with Fig. 8(b), it is evident that there exists a range of reactive fluids that can enhance the heat delivered to the heat sink by >80 % compared to inert fluid *A*, while penalizing the COP by <20 %.

For certain reactive fluids, external heat exchange with the heat sink and source exclusively occurs during the isothermal compression and expansion processes. No additional heat sink or source is required during the isochoric processes. However, for these fluids, the COP still falls short of reaching the COP observed in inert fluids. Although the heat exchange in the internal regenerator is complete ($q_{23} = q_{41}$), the chemical reaction in the system leads to heat exchange across a finite temperature difference and introduces irreversibility. This irreversibility can be quantified by the entropy generated in the internal adiabatic regenerator calculated according to Eq. (14), as presented in Fig. 9.

$$s_{gen.reg} = \Delta s_{hot\ stream} + \Delta s_{cold\ stream} \tag{14}$$

Where $s_{gen.reg}$ represents the specific entropy generated in the generator, $\Delta s_{hot\ stream}$ is the change in the specific entropy of the hot stream of the regenerator (outlet minus inlet), and $\Delta s_{cold\ stream}$ is the change in the specific entropy of the cold stream.

To better understand the effect of the chemical reaction on the entropy generation in the internal regenerator, the heat exchanged during isochoric processes, and the resulting COP of the cycle, the temperature-heat ($T-q$) diagrams for six fluids are presented in Fig. 10. These include the two inert fluids, A_2 and *A*, as well as four reactive fluids numbered (1) through (4), all of which are identified in Fig. 9.

Reactive fluid (1) in Fig. 9 is characterized by a COP that is comparable to that of inert fluids *A* and A_2. The total heat released during isochoric cooling, q_{23}, and the total heat absorbed during isochoric heating, q_{41}, are slightly different. This can be observed in Fig. 10(c). For this fluid, the entropy generation in the internal regenerator is negligible, where the temperature difference between the two streams during heat exchange is minor.

Observing Fig. 10(d), in the case of Reactive Fluid (2), q_{41} is greater than q_{23}. An additional external heat source is required during isochoric process (4–1) in order to heat the fluid to T_H, penalizing the COP of the cycle. Conversely, q_{23} is greater than q_{41} in the case of Reactive Fluid (3), as presented in Fig. 10(e). An additional external heat source is required during isochoric cooling in order to cool the hot stream to T_C.

On the other hand, external heat transfer exclusively takes place during isothermal compression and expansion in the case of Reactive Fluid (4). The heat exchange in the internal regenerator is complete ($q_{23} = q_{41}$), as presented in Fig. 10(f). Therefore, the reduced COP of this fluid can be attributed to the irreversibility of the regenerator due to heat exchange across a finite temperature difference, in contrast to the case of inert fluids A_2 and *A*, as displayed in Figs. 10(a) and 10(b), respectively.

4. Conclusion

In this work, the performance of a regenerative Stirling heat pump operating with a chemically reactive–rather than inert–working fluid is assessed. A range of theoretical reactive gaseous mixtures, modeled on the basis of the ideal gas mixture thermodynamic model, is investigated. All fluids are characterized by the equilibrated chemical reaction $A_{2(g)} \rightleftarrows 2A_{(g)}$, and each fluid is identified by a unique set of the reaction coordinates: standard entropy change of reaction ($\Delta_R S^\circ$) and standard enthalpy change of reaction ($\Delta_R H^\circ$). The thermodynamic properties of each fluid are evaluated throughout the reverse Stirling cycle, and, consequently, the overall performance (COP) of the heat pump is calculated. The results are benchmarked against those of comparable inert working fluids (*A* and A_2).

It is observed that for a wide range of reactive fluids, the heat exchange in the internal regenerator is incomplete; the total heat released during isochoric cooling and the total heat absorbed during isochoric heating are not equivalent. Consequently, additional external heat sink during isochoric cooling, source during isochoric heating, or both are needed in the cycle, penalizing the COP of the heat pump.

However, due to the reactive nature of the fluid, for certain reactive fluids, the exothermic reaction during isothermal compression significantly increases the thermal energy supplied to the heat sink. Up to 269 % increase in the specific heat supplied to the heat sink, q_{comp}, and thermal energy density per unit maximum volume, q_{comp}/v_4, can be achieved, while penalizing the COP by <20 %.

In the case of reactive fluids where the heat exchange in the regenerator is complete, some of these fluids exhibit behavior similar to inert fluids during heat exchange in the regenerator, yet provide an increased heat supply to the heat sink during isothermal compression due to the exothermic reaction. The latter offer a comparable COP to that of *A* and A_2. Furthermore, they are characterized by a favorable endothermic reaction during isochoric cooling and a favorable exothermic reaction during isochoric heating. However, other fluids are characterized by pronounced unfavorable chemical reactions during the isochoric processes, leading to irreversibility in the internal regenerator due to heat transfer across a finite temperature difference and penalizing the COP, even when regeneration is complete.

The next steps of the project involve exploring and assessing real chemically reactive working fluids in thermodynamic cycles, as well as experimentally validating the results.

CRediT authorship contribution statement

Aya Barakat: Writing – original draft, Visualization, Software, Methodology, Conceptualization. **Jean-Noël Jaubert:** Writing – review & editing, Supervision, Methodology, Conceptualization. **Philippe Arpentinier:** Writing – review & editing, Methodology. **Pascal Tobaly:** Writing – review & editing, Methodology. **Silvia Lasala:** Writing – review & editing, Validation, Supervision, Project administration, Methodology, Funding acquisition, Conceptualization.

Declaration of competing interest

The authors declare that they have no known competing financial interests or personal relationships that could have appeared to influence the work reported in this paper.

Acknowledgments

This work has received funding from the European Research Council (ERC) under the European Union's Horizon Europe research and innovation program (grant agreement No 101040994).

References

Ahmadi, M.H., Ahmadi, M.-A., Mohammadi, A.H., Mehrpooya, M., Feidt, M., 2014. Thermodynamic optimization of Stirling heat pump based on multiple criteria. Energy Convers. Manag. 80, 319–328. https://doi.org/10.1016/j.enconman.2014.01.031. Apr.

Ahmadi, M.H., Ahmadi, M.A., Bayat, R., Ashouri, M., Feidt, M., 2015. Thermo-economic optimization of Stirling heat pump by using non-dominated sorting genetic algorithm. Energy Convers. Manag. 91, 315–322. https://doi.org/10.1016/j.enconman.2014.12.006. Feb.

Barakat, A., Lasala, S., Arpentinier, P., Jaubert, J.-N., 2022. The original and impactful exploitation of chemical energy in heat pumps. Chem. Eng. J. Adv. 12, 100400. https://doi.org/10.1016/j.ceja.2022.100400. Nov.

Barakat, A., Lasala, S., Arpentinier, P., Tobaly, P., Jaubert, J.-N., 2024. Understanding the thermodynamic effects of chemically reactive working fluids in the Stirling engine. Energy Convers. Manag.: X, 100573. https://doi.org/10.1016/j.ecmx.2024.100573. Mar.

Barreno, I., Costa, S.C., Cordon, M., Urrutibeascoa, I., Gomez, X., Mateos, M., 2014. Dynamics of an oscillating Stirling heat pump. Appl Energy 136, 704–711. https://doi.org/10.1016/j.apenergy.2014.09.080. Dec.

Cheng, C.-H., Yang, H.-S., Chen, H.-X., 2020. Development of a beta-type Stirling heat pump with rhombic drive mechanism by a modified non-ideal adiabatic model. Int. J. Energy Res. 44 (7), 5197–5208. https://doi.org/10.1002/er.5258.

D. Haywood, "Investigation of Stirling-type heat-pump and refrigerator systems using air as the refrigerant.," University of Canterbury, 2004. Accessed: Oct. 27, 2023. [Online]. Available: http://hdl.handle.net/10092/2566.

IEA, 2021. Renewables 2021. IEA, Paris. Accessed: Apr. 23, 2024. [Online]. Available: https://www.iea.org/reports/renewables-2021.

IEA, 2022. The Future of Heat Pumps. IEA, Paris. Nov.[Online]. Available: https://www.iea.org/reports/the-future-of-heat-pumps.

Kemp, H.R., 1987. The effect of temperature and pressure on equilibria: A derivation of the van't Hoff rules. J Chem Educ 64 (6), 482. https://doi.org/10.1021/ed064p482.

Khan, U., Zevenhoven, R., Tveit, T.-M., 2020. Evaluation of the environmental sustainability of a stirling cycle-based heat pump using LCA. Energies 13 (17), 4469. https://doi.org/10.3390/en13174469. Jan.

Koudriavtsev, A.B., Jameson, R.F., Linert, W., 2011. The Law of Mass Action. Springer Science & Business Media.

Kovtun, I.M., Naumov, A.N., Nesterenko, V.B., 1967. Stirling cycle using a dissociating gas. Akademiia Navuk BSSR, Vestsi, Seryia Fizika-Tekhnichnykh Navuk (1), 52–57.

Kowalski, S., Abuheiba, A., Jewett, R., Gluesenkamp, K., Nawaz, K., 2022. Efficiency and Capacity Performance of a Stirling-Cycle Water-To-Water Heat Pump. Oak Ridge National Lab. (ORNL), Oak Ridge, TN (United States). Jul.Accessed: Nov. 02, 2023. [Online]. Available: https://www.osti.gov/biblio/1885361.

Lasala, S., Privat, R., Herbinet, O., Arpentinier, P., Bonalumi, D., Jaubert, J.-N., 2021. Thermo-chemical engines: Unexploited high-potential energy converters. Energy Convers. Manag. 229, 113685. https://doi.org/10.1016/j.enconman.2020.113685. Feb.

Lasala, S., et al., 2024. Application of thermodynamics at different scales to describe the behaviour of fast reacting binary mixtures in vapour-liquid equilibrium. Chem. Eng. J. 483, 148961. https://doi.org/10.1016/j.cej.2024.148961. Mar.

Lasala, S., 2022. Reactive fluids for intensified thermal energy conversion (REACHER). European Research Council [Online]. Available: https://www.univ-lorraine.fr/erc-reacher/.

Metwally, M.M., Walker, G., 1977. Stirling engines with a chemically reactive working fluid—some thermodynamic effects. J. Eng. Power 99 (2), 284–287. https://doi.org/10.1115/1.3446287. Apr.

Penswick, L., Olan, R.W., Williford, I., Draney, S., Buchholz, G., 2014. High-capacity and efficiency stirling cycle cryocooler. Cryocoolers 18.

Radebaugh, R., 2009. Cryocoolers: the state of the art and recent developments. J. Phys.: Condens. Matter 21 (16), 164219. https://doi.org/10.1088/0953-8984/21/16/164219. Mar.

Tekin, Y., Ataer, O.E., 2010. Performance of V-type Stirling-cycle refrigerator for different working fluids. Int. J. Refrig. 33 (1), 12–18. https://doi.org/10.1016/j.ijrefrig.2009.08.011. Jan.

Tyagi, S.K., Kaushik, S.C., Salhotra, R., 2002. Ecological optimization and performance study of irreversible Stirling and Ericsson heat engines. J. Phys. D: Appl. Phys. 35 (20), 2668. https://doi.org/10.1088/0022-3727/35/20/330. Oct.

Tyagi, S.K., Chen, J., Kaushik, S.C., 2004. Thermoeconomic optimization and parametric study of an irreversible Stirling heat pump cycle. Int. J. Therm. Sci. 43 (1), 105–112. https://doi.org/10.1016/S1290-0729(03)00101-7. Jan.

U.S. Energy Information Administration, 2024. Residential Energy Consumption Survey (RECS). Accessed: Apr. 22, 2024. [Online]. Available: https://www.eia.gov/consumption/residential/.

Wang, R., Hu, J., Jia, Z., Zhang, L., Luo, E., 2021. Study on the temperature adaptability of free-piston Stirling heat pump. Energy Convers. Manag. 249, 114864. https://doi.org/10.1016/j.enconman.2021.114864. Dec.

Wolgemuth, C.H., 1934. The Use of a Chemically Reactive Gas in a Closed Stirling Cycle. The Ohio State University.